

IMPACT OF BLASTING AT TUNNEL FACE ON AN EXISTING ADJACENT TUNNEL

V.K. Dang¹, D. Dias^{2,3}, N.A. Do¹, T.H. Vo¹

¹Hanoi University of Mining and Geology, Faculty of Civil Engineering, Hanoi, Vietnam

²School of Automotive and Transportation Engineering, Hefei University of Technology, Hefei, China

³Grenoble Alpes University, Laboratory 3SR, Grenoble, France

*Corresponding Author, Received: 12 Dec. 2017, Revised: 22 Dec. 2017, Accepted: 20 Jan. 2018

ABSTRACT: Experimental and numerical research of the effect of blasting vibrations during tunneling on surrounding structures (rock mass, existing tunnels, buildings, etc.) was widely studied in recent years. However, the effect of blasting vibration from a new tunnel on an existing adjacent tunnel is still unclear. A few researches were carried out to study the relationship of the observed Peak Particle Velocity (PPV) on the lining areas along the existing tunnel direction, due to either the lack of in situ test data or the difficulty in conducting field tests, particularly for tunnels that are usually old and vulnerable after several decades of service. This paper introduced two dimensional and three dimensional numerical with field data investigations on the effect of tunnel face blasting on the surrounding rock mass and on an existing adjacent tunnel along the existing tunnel direction. The Croix-Rousse tunnel project in Lyon (France) was adopted as a case study. The derived results allow predicting the tunnel lining damage areas under the impact of blast loads.

Keywords: Peak particle velocity, Blasting vibration, Tunnel blasting, Numerical model, Twin tunnels

1. INTRODUCTION

The effect of blasting from the new tunnel on the existing tunnel was studied in the past using a variety of approaches: physical model testing, field observations, empirical/analytical methods and finite element modeling. Some researches were carried out using physical models to study the effect of blasting vibration on an existing tunnel [2], [3]. Smith et al presented the results of experimental studies carried out at small scale into the propagation of blast waves along straight tunnels roughened by means of different-sized roughness elements fixed along the two model tunnels sides. The results indicated that the use of rough-walled tunnels could provide an efficient protective solution to a sensitive structure. Khosrow studied the impact of joints and discontinuities on the blast-response of tunnels using physical modeling at 1-g [3]. However, the physical model testing method was just used to analyze the effect of blasting vibrations due to a blast at the tunnel face.

The theoretical researches are relatively scarce and mainly adopt the integral equation method and the ray theory method [4]. In addition, [5] used a closed-form transient solution for the case of circular tunnels and blasting loading. In the research of [6], a theoretical method to predict the underground tunnel behavior considering the peak particle velocity (PPV) and the stress distribution is also presented. The influence of the explosion-

induced wave on an adjacent tunnel is explicitly considered in order to evaluate tunnel stability. However, this method usually uses a simple tunnel shape such as a circular tunnel and the obtained results are limited.

The influences of blasting vibration on underground structures have also been studied using field experiments [7] - [12] and numerical simulations [13] - [21]. The results obtained by numerical simulation can be compared with field experiments during all the blasting time period or in terms of magnitude values. The comparison of time results obtained with these two methods is usually used in the case of a sole explosion such as in metro due to terrorist acts [12], [13]. A comparison of magnitude values can be used in the case of blasting shots with time delay such as explosions at a tunnel face during tunnel excavation by blasting method [16], [18-21].

Previous publications have indicated that the strongest vibrations of the existing tunnel lining occur on the side closest to the blasting center, and are proportional to the maximum segmental explosive charge instead of the total charge. Rock masses with harder rock and fewer discontinuities seem to contribute to stronger tunnel vibrations than softer rock and more discontinuities. This fact induces greater risks for tunnels in 'high-quality' rock masses [18]. However, a few researches were carried out to study the relationship of the observed PPV on the lining areas along the existing tunnel direction, due to either the lack of in situ test data

or the difficulty in conducting field tests, particularly for tunnels that are usually old and vulnerable after several decades of service. It is therefore necessary to conduct both experimental and numerical research to improve the knowledge of the blasting impact on the lining areas along the existing tunnel direction. The main objective of this research is thus to analyse such problems by comprehensive use of in situ testing, namely the PPV, and numerical simulations in which parameters are determined from laboratory tests.

In this paper, a research based on real scale blasting tests performed on the Croix Rousse tunnel (Lyon, France) is presented. This tunnel was excavated close to an existing tunnel. 2D and 3D numerical models of the real site were conducted using the finite element software Abaqus/Explicit. The dynamic responses of the tunnel concrete lining and of the surrounding rock mass subjected to blasting vibrations were analyzed. The impact of blasting at the tunnel face on the existing adjacent tunnel was considered. Measurements during blasting in the new tunnel were performed to verify the stability of the lining in the existing tunnel. These field data were used to validate the 2D and 3D numerical models developed in this research. The real parameters of blasting in Croix-Rousse tunnel were considered. A parametric study was then conducted using these 2D/3D models to evaluate the most dangerous section in the existing tunnel. The idea was to check the lining areas along the existing tunnel direction which can be partially damaged. The numerical results indicated that the concrete lining in the existing tunnel has not suffered significant damages.

2. THE CROIX-ROUSSE TUNNEL

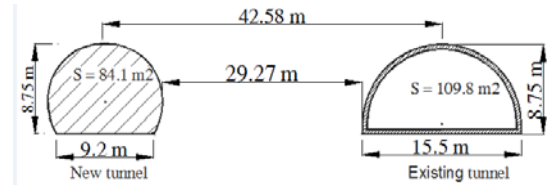
2.1 Site Description

The Croix-Rousse tunnel is located in Lyon, France, between the Rhône and the Saone rivers. The length of the tunnel is 1757 m with a cross-section area of 84.10m². A new tunnel was excavated in parallel of the existing one. The distance wall to wall between these two tunnels is of around 29.27m (Fig. 1.a). The cover depth of the tunnels varies between 70 and 100m (Fig. 1.b).

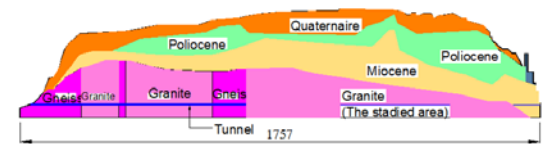
2.2 Geology Conditions

The tunnels were excavated through granite and gneiss layers with uniaxial compressive strengths higher than 100MPa, using drilling and blasting method. The dynamic parameters of the rock were determined on the basis of the Split Hopkinson pressure bar tests [22], [23]. During laboratory tests, the pressure was increased until the rupture of the rock sample is observed. The

rupture pressure value of 3.5 bars is indicated in Fig. 2. Dynamic parameters of the rock mass are listed in Table 1.



a. Tunnels geometry



b. Geology of the site

Fig.1 Tunnels geometry and geology conditions along the tunnel (b)





Pressure (bar)	1.0	2.0	3.0	3.5
Observations	No damage	Shards at the end	Large pieces at the end	Rupture
Pictures				

Fig.2 Results of the Split Hopkinson pressure bar tests on a rock sample (Granite)

Table 1 Dynamic parameters for the rock mass

Parameters	Unit	Value
Density (γ_r)	kg/m ³	2650
Dynamic Young's modulus (E_r)	GPa	60
Poisson's ratio (ν_r)	-	0.25
Friction angle (ϕ_r)	degrees	54
Dilation angle (ψ_r)	degrees	4
Cohesion (C_r)	MPa	23
Compressive strength (σ_{cr})	MPa	120
Dynamic tensile strength (σ_{tr})	MPa	5.70
Shear wave velocity	m/s	3800

2.3 Blasting Parameters

On the tunnel face, eight blast hole groups were set up: I-cut holes, three stopping grounds, two wall holes grounds and lifter holes. Blasthole groups at the tunnel face are presented in Fig. 3.

Due to the importance of the existing tunnel and of the structure on the ground surface, the definition of the upper limit of the PPV was required by both the owner and the designer in order to reduce the impact of the new tunnel excavation.

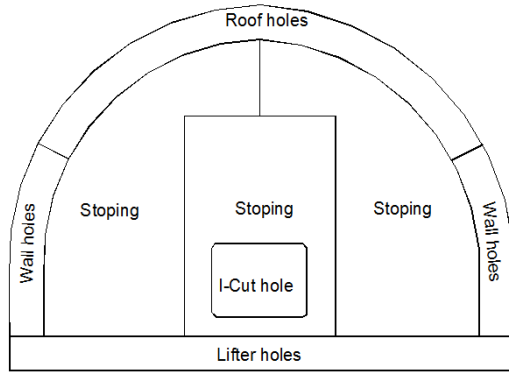


Fig.3 Blasthole groups on the tunnel face in the Croix-Rousse tunnel

The result of blasting vibrations induced in concrete tunnel lining is presented in Table 2. According to measuring data, frequency of blasting vibration during Croix-Rousse tunnel excavation varies from 1Hz to 250Hz. Also according to measuring data, two important frequencies of 10 Hz and 100 Hz, which correspond to the largest vibration velocity, were adopted for the parametric study.

3. IN SITU MONITORING RESULTS

The blasting vibrations induced in the existing tunnel during the excavation of the new Croix-Rousse tunnel were monitored using sensors of Geophone type. The sensors (A, P and T as seen in Fig. 4) were embedded in the concrete lining along the tunnel axis. Results of the PPV values are monitored in three directions, including the transverse direction, the vertical direction and the longitudinal direction of the tunnel. The maximum value of the three orthogonal components (x, y, z) are presented in Table 2.

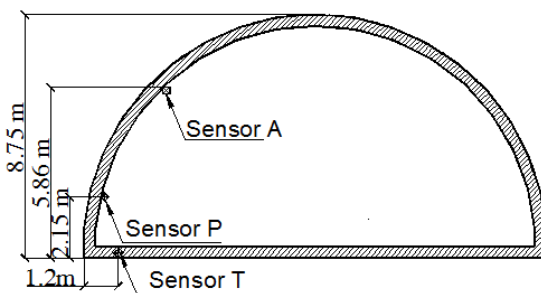


Fig. 4 Location of sensors in the existing tunnel

4. NUMERICAL SIMULATIONS

Numerical simulations were performed using the Finite Element Method with the Abaqus/Explicit 6.11-2 software [1]. Both 2D and 3D models were used in this research. Using 2D models permits to validate the mesh and

investigate some parameters of the model. For the propagation problem, the 3D model gives results which are better than the 2D model if compared with the monitoring data. Indeed, the blasting energy was absorbed in the 3D model by the rock mass in closer conditions to the real condition. Whereas, blasting energy was absorbed in the cross-section in the 2D plane strain model.

Table 2 Monitoring data of blasting velocity

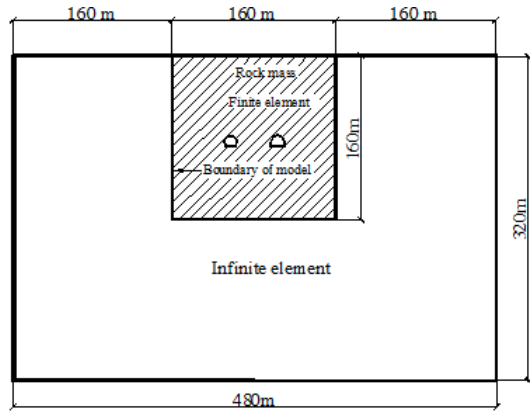
Order number of blasting	Explosion weight, Q_{max} (kg)	V_{max} (mm/s)
230	544.0	3.58
231	574.5	8.99
232	647.0	12.12
233	662.0	15.36
234	1153.0	14.59
235	870.0	10.08
236	871.0	7.21
239	849.0	5.69

4.1 Description of the Numerical Models

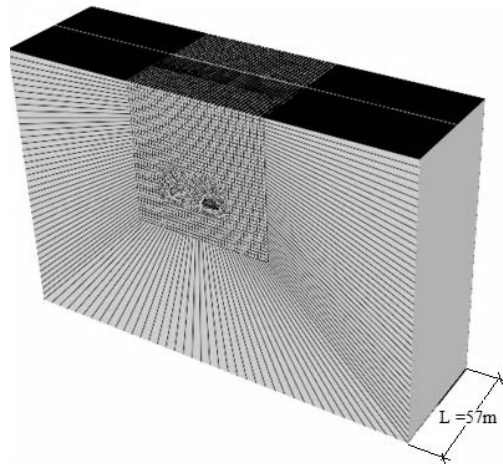
Numerical models were carried out to investigate the blast vibration of the newly excavated tunnel close to the existing one. A rock mass of 160 m in height and 160 m in width is considered. A concrete tunnel lining of 0.75 m in average thickness is taken into account. The existing tunnel has a vaulted roof and vertical walls. The radius of the arch is 8.05m and the height of the vertical wall is equal to 1.0m. The newly excavated tunnel is a horseshoe arch with the radius of 5.55 m. The distance between the two tunnels from center to center is equal to 42.6m. The 2D model geometry is presented in Fig.5.

The transversal section of the 3D model is the same as the 2D one. A parametric study on the length L was done (L= 28m, 42m, 57m, 84m, 108m) [35]. Results indicated that when this length is equal to 57m, the peak particle velocity value is constant inside the tunnel lining. A model length of L=57m was then considered for the following study [35]. This length was chosen for the parametric study purpose. The length of an excavation step is equal to 4.0 m.

The numerical model consists of 388742 elements, including 375062 finite elements of C3D8R type and 13680 infinite elements of CIN3D8 type. The minimum size for the finite elements is equal to 0.34m and the maximum to 0.65m. The maximum dimension of elements in the model was checked according to Kuhlemeyer and Lysmer (1973). The absorbent boundaries are placed at the border between the finite and the infinite elements.



a) 2D numerical model



b) 3D numerical model

Fig. 5 Geometry of the numerical models

4.2. Validation of the mesh: Raleigh velocity

The velocity of the Rayleigh wave is used to validate the numerical model mesh (Fig. 6).

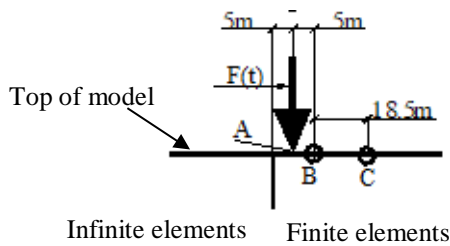


Fig. 6 Location of the applied time-dependent force and of the monitored points

A time-dependent force was applied to a point at a distance of 5m from the left boundary. The stress magnitude was equal to 1500 GPa (this value was randomly taken), the relation between load and time can be seen in Fig. 7 and Eq. (1):

$$F(t) = 1.5 \cdot 10^{12} \cdot f(t) \quad (1)$$

In order to validate the mesh, the velocity of the Rayleigh wave propagation is considered. The theoretical velocity of the Rayleigh wave is calculated using the Bergmann-Viktorov [36] formula:

$$V_R = \frac{0.87 + 1.12\nu}{1 + \nu} \cdot V_S \quad (2)$$

where: ν is the Poisson's ratio, V_S is the S-wave velocity:

$$V_S = \sqrt{\frac{G}{\rho}} = \sqrt{\frac{E}{2(1 + \nu)}} \quad (3)$$

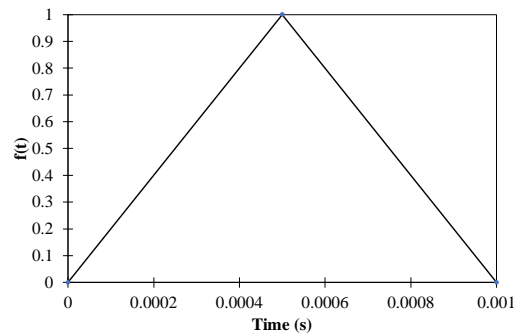


Fig. 7 Time pressure profile

The V_S wave was calculated using the above formula and compared to the finite element numerical one. A difference of less than 2% was found which permits to conclude that the mesh is convergent.

4.3 Boundary Conditions

For the 2D models, coupled finite-infinite elements were used including CPE4R and CINPE4 typed elements. The top surface is free, while for the three other surfaces non-reflecting boundaries were used and assigned using infinite elements CINPE4.

For the 3D models, finite and infinite elements which are CD8R and CIN3D8, respectively, were also used. The three surfaces of the numerical model in the transverse direction and in the vertical direction were assigned as non-reflecting boundaries. The displacement in the tunnel axis orientation was assumed to be zero. The reflection conditions at boundaries of 3D model are similar to those of 2D model.

4.4 Damping Matrix

This research used Rayleigh damping method. The damping matrix of the given system is a linear combination of the mass matrix and stiffness matrix, i.e. as Eq. (4):

$$[C] = \alpha[M] + \beta[K] \quad (4)$$

where: α and β are the damping constants depending on the energy damping properties of the materials. Their values can be calculated by the following equations:

$$\alpha = \frac{2\omega_1\omega_2(\xi_1\omega_2 - \xi_2\omega_1)}{\omega_2^2 - \omega_1^2} \quad (5)$$

$$\beta = \frac{2(\xi_1\omega_2 - \xi_2\omega_1)}{\omega_2^2 - \omega_1^2}$$

where: ω_1 is the first tone vibration frequency, and ω_2 is the maximum tone vibration frequency of important interest (usually $f_1 = \omega_1/2\pi$ and $f_2 = \omega_2/2\pi$). The factors of modal damping ξ_1 and ξ_2 correspond to values of frequencies ω_1 and ω_2 . The damping ratio is associated to the j mode of vibration through the expression.

$$\xi_j = \frac{\alpha}{2\omega_j} + \frac{\beta\omega_j}{2} \quad (6)$$

4.5 Blasting Load Model

When the explosion is detonated, the explosion energy is released under wave types. A part of the explosion energy is applied on the tunnel boundaries. There are two typical categories of detonation, namely, ideal and non-ideal detonation. The ideal detonation profile corresponds to an emulsion-type explosive where the peak pressure rise time is very short and the post-peak pressure drop is steep. The non-ideal detonation profile corresponds to an ANFO type explosive where the rise time for the peak blast-hole pressure is longer and the post-peak pressure drop is much slower than in the case of the emulsion type explosive [14].

For the Croix-Rousse tunnel, emulsion explosive was used to excavate the tunnel. The ideal detonation shape was chosen to calculate the blasting loads. These blasting groups are usually detonated at different times using delay electric detonators in the tunnel face. In this study, blasting has been simulated into eight separated shots with the same peak blast-hole pressure (see Fig. 8). Blasting loads time history curve of each shot is presented in Fig. 8. Blasting pressure is radially applied to the all the tunnel boundaries and it is not applied to the tunnel face.

Generally, the detonation pressure is not fully charged on the blast-hole due to the existence of an empty space between the explosive column and the blast-hole wall. The following calibration equation was used to estimate the blast-hole pressure P_B [15]:

$$P_B = P_d \left(\frac{d_c}{d_h} \right)^3 \quad (7)$$

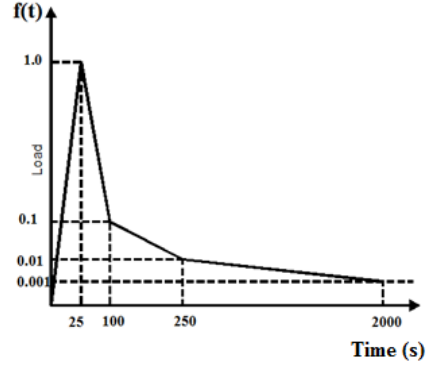


Fig. 8 Optimized pressure-time profiles of different explosive characteristics simulated in this study [14]

where: P_B is the blast-hole pressure considering decoupling (kPa; d_c and d_h are diameters of explosive and blast-hole (mm), respectively; P_d is the peak borehole pressure estimated using the following equation of [24] (kPa):

$$P_d = \frac{4.18 \times 10^{-7} \times SG_e \times V_e^2}{1 + 0.8 SG_e} \quad (8)$$

where: SG_e is the density of explosive (g/cm^3); V_e is the detonation velocity of explosive (ft/s).

The non-electric millisecond delay detonators labeled MS1÷MS8 are adopted. Their delay times are listed in Table 3.

Table 3 Time interval of every shot

Series of detonator (1)	MS 1	MS 2	MS 3	MS 4
Time of peak pressure from beginning (ms) (2)	0.025	27±10	54±10	156±10
(1)	MS 5	MS 6	MS 7	MS 8
(2)	250 ±10	360±10	560±10	760±10

The peak pressure value of each shot was calculated using Eq. (7) and resulted in $P_B = 7.48 \times 10^6$ kPa. The blasting load applied on the tunnel boundaries $P(t)$ is estimated by Eq. (9):

$$P(t) = P_B f(t) = 7.48 \times 10^6 f(t); \text{ kPa} \quad (9)$$

4.6 Constitutive model and parameters of ground

The granite rock mass was modeled using the linear elastic-perfectly plastic constitutive model (with Mohr-Coulomb failure criterion). The dynamic parameters of the rock mass see in Table 1. The concrete tunnel lining was simulated using

the concrete damaged plasticity constitutive model. Parameters of concrete tunnel lining under dynamic load see in Table 4.

5. PARAMETRIC STUDY

In order to follow the velocity in the tunnel lining during blasting, some sensors named A, P, T as seen in Fig.4 were installed in the concrete lining of the existing tunnel. A parametric study is carried on the 2D numerical model. The investigation result is used for calculating on the 3D model.

Table 4 Dynamic parameters of the concrete lining

Parameters	Unit	Value
Thickness (d)	m	0.75
Density (γ_c)	kg/m ³	2400
Young's Modulus (E_c)	GPa	35.00
Poisson's ratio (ν_c)	-	0.200
Compressive strength (σ_{cc})	MPa	35.00
Tensile strength (σ_{tc})	MPa	2.90

5.1 Influence of the Materials Damping Ratio

For geological materials (e.g., soils, rock), damping ratio commonly falls in the range of 2% to 5% [26]. Two frequencies of 10Hz and 100Hz were used to determine the damping constants material in Eq. (5). The damping ratio of concrete lining was set equal to 4%. Several values of the damping ratio applied to the rock mass were considered in the 2D numerical models: $\xi = 3\%$, $\xi = 4\%$, and $\xi = 5\%$.

The numerical results presented in Fig. 9 indicated that when the damping ratio increases, the PPV generally decreases. On the basis of the comparison between the monitored data and the numerical results, the obtained results for $\xi = 3\%$, $\xi = 4\%$ and $\xi = 5\%$ are very different. The PPV obtained with damping ratio 3% is larger than the one obtained with a damping ratio of 4%. The average difference between them is about 18.2%. It can be explained by the fact that the smaller the damping ratio, the greater the blasting energy absorbed by the rock mass. The PPV obtained with the damping ratio equal to 5% is closer to the one obtained by the monitored result. A damping ratio equal to 5% was therefore adopted and used in the following study (Fig. 9).

5.2 Influence of the Rock Mass Constitutive Model

In order to highlight the effect of the rock mass constitutive model under blasting load, the

behavior of the rock mass has been assumed to be linear-elastic and elastic-perfectly plastic. The latter constitutive model of the rock mass is based on the Mohr-Coulomb failure criterion.

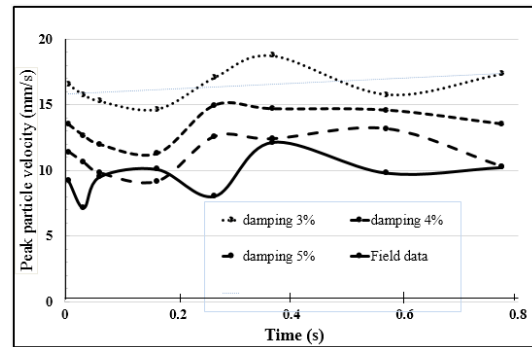


Fig. 9 Effect of the Rayleigh damping on the PPV values (sensor A)

The results presented in Table 5 and Fig. 10 show an insignificant difference between the numerical results and the monitored data in terms of the PPV in the tunnel lining when the Mohr-Coulomb constitutive model is used. On the other hand, the PPV in the tunnel lining observed with the linear-elastic constitutive model is about 50% greater than the monitored one (Fig.10). It is reasonable to conclude that the linear-elastic constitutive model is not sufficiently complex and is then not able to study the effect of blast vibration.

Table 5 Peak particle velocity (mm/s) obtained with the numerical model and the monitored data

Time (s)	Linear elastic model (1)	Mohr-Coulomb model (2)	Field data (3)	Difference (%) (1)/(3)	Difference (%) (2)/(3)
t=0.0064s	22.743	11.422	9.230	0.59	0.19
t=0.033s	20.713	10.619	7.179	0.65	0.32
t=0.061s	19.291	9.816	9.523	0.51	0.03
t=0.163s	24.342	10.543	10.100	0.59	0.04
t=0.264s	29.168	12.584	8.058	0.72	0.36
t=0.366s	27.617	12.407	12.161	0.56	0.02
t=0.568s	37.356	13.176	9.816	0.74	0.26
t=0.771s	50.356	11.422	10.246	0.59	0.19

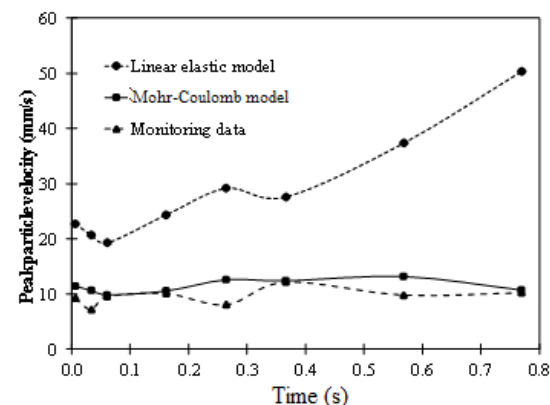


Fig. 10 Influence of rock mass constitutive model

6. EFFECT OF BLASTING LOADS IN THE NEW TUNNEL

In this section, 3D numerical models were used to investigate the effect of blasting load from the new tunnel on the existing tunnel considering various distances in the longitudinal direction of the tunnel. The layout of the two tunnels is presented in Fig. 11. D represents the distance from the section in the existing tunnel to the tunnel face of the new tunnel. The numerical results indicate that the biggest particle velocity induced in the tunnel lining of the existing tunnel is obtained when the section is closer to the blasting location (the case of D = 0 in Fig. 11).

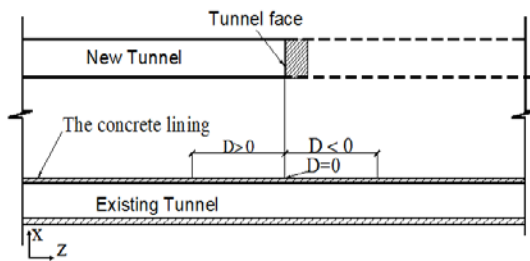


Fig.11 Layout of two tunnels

In other words, the smaller the distance from the blasting location in the new tunnel, the more dangerous state of the concrete lining in the existing tunnel. Figure 12 and Table 6 show a comparison between the numerical results and the monitoring data in terms of PPV induced in the tunnel lining. Numerical results obtained with the 3D model are closer to the monitoring data (Fig.12). This may be concerned with the fact that the blasting energy in the 3D model is also absorbed by the rock mass in the longitudinal direction. This phenomenon is not considered in the 2D model, a 3D model is therefore necessary to be used.

Table 6 Comparison between 2D and 3D numerical simulations with monitoring data

D (m)	Field data (mm/s)	3D model results (mm/s)	Difference between (1) and (2) (%)	2D model results (mm/s)
(1)	(2)	(3)	(4)	
-12	3.58	2.784	22.222	
-8	8.99	6.242	30.562	
-4	12.12	14.960	23.433	
0	15.36	15.532	1.126	17.357
4	10.08	8.094	19.700	
8	7.21	7.190	0.271	
12	5.69	5.623	1.163	

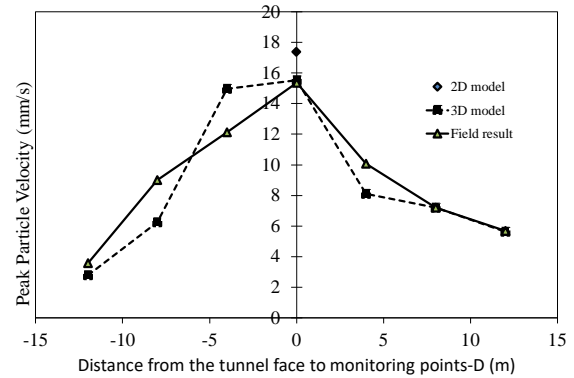


Fig. 12 Comparison between 2D and 3D numerical simulations with monitoring data

7. STABILITY OF CONCRETE TUNNEL LINING

In order to estimate the failure state of the tunnel lining under the blasting vibrations impact, two criterions were used including: (1) the threshold PPV and/or (2) the dynamic tensile strength. The threshold velocity was determined by using the DIN4150 standard [27]. The allowable level of PPV depends on the type of tunnel structures, and is specified in the design regulations [27]. The typical frequency range of the underground blast-induced vibrations is in the range between 50 to 100 Hz. Accordingly, threshold velocities of about 40 to 100 mm/s with frequency changing from 1 to 100 Hz are considered by the DIN4150 standard. In this research, the PPV measured by the sensors was equal to 15.53 mm/s (Table 7) which is smaller than the threshold velocity calculated by the DIN4150 standard (minimum 40 mm/s). In addition, the maximum tensile stress induced in the lining of the existing tunnel is about 2.69 MPa which is under the dynamic tensile strength of 2.9 MPa used for the concrete material [28]. It is, therefore, reasonable to conclude that the lining in the existing tunnel is stable under the impact of blasting vibration from the new tunnel.

To evaluate the blasting parameters influence which caused damage to the existing tunnel lining, a parametric study was conducted. The blasting load acting on the new tunnel perimeter was increased gradually from the actual value used in Croix-Rouge tunnel to values at which damages in the existing tunnel lining can occur. Keeping the time function of blasting load (see Eq. (9)), damages in the existing tunnel lining were observed when the blasting load is equal to 1.5 times the previous value as seen in Fig.13.

The most dangerous zone in the existing tunnel lining with the highest density of damaged elements is in the section which is parallel to the new tunnel excavation face (Fig. 13b, c).

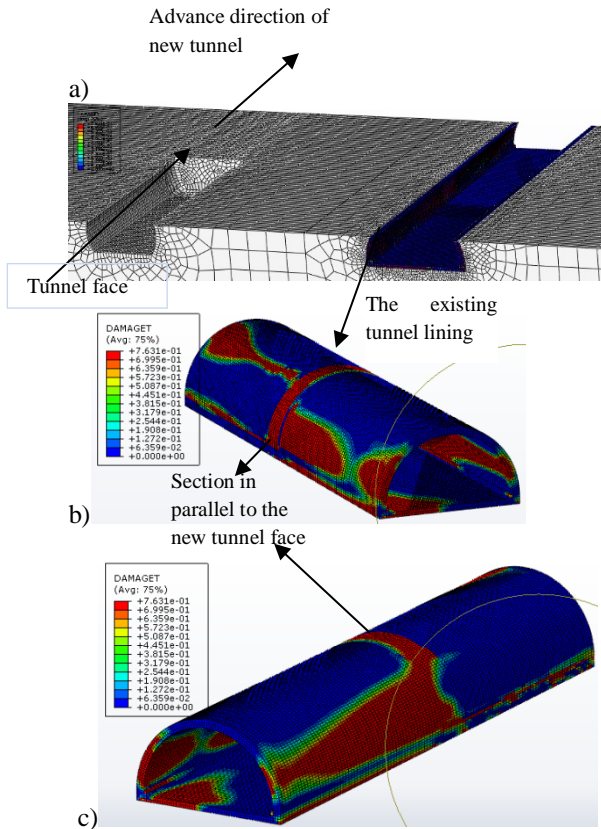


Fig. 13 Damaged zones in the existing tunnel lining at the time equal to 0.00332s: a) Location of the two tunnels; b) Side facing to the new tunnel; c) Side not facing the new tunnel.

It is also interesting to note that in the existing tunnel, damaged elements were predominately observed at the tunnel walls on both sides of the lining zones which are behind the new tunnel face. Less damaged zones are observed at the left shoulder of the existing tunnel lining sections which are in front of the new tunnel face (see Fig. 13b, c). This damaged zone ranges difference in the existing tunnel lining and at the two sides of the new tunnel face may be concerned by the effect of the blasting wave propagation from the new tunnel to the existing tunnel along the new tunnel direction.

8. CONCLUSION AND DISCUSSION

This paper presents a numerical study that investigates the impact of blasting on an existing adjacent tunnel. Analyses were carried out using 2D and 3D numerical models. A good agreement between the numerical results and the monitoring data was found. Several conclusions can be drawn as follows:

- The PPV is inversely proportional to the damping ratios. On the basis of the comparison between the monitoring data and the numerical results, a damping ratio of 5% was adopted.

- A significant influence of the soil constitutive model of the rock mass behavior under blasting loads was indicated. It is reasonable to conclude that a linear elastic constitutive model is not realistic to simulate the effect of blast vibrations.

- The 3D numerical model results indicate that the largest particle velocity induced in the tunnel lining is obtained at the section closer to the blasting location. In other words, the smaller the distance from the blasting location in the new tunnel, the more dangerous state of the tunnel lining in the existing tunnel.

- The numerical results derived from the 3D models are in a good agreement with monitoring data. The 2D models are not able to simulate all the 3D effect of the blasting loads.

- The lining of the existing tunnel is stable under the impact of blasting vibrations with the maximum explosion used for the Croix-Rousse tunnel. Damages in the existing tunnel lining can appear for blasting loads 1.5 times higher than the previous ones.

- The rock mass close to the new tunnel is drastically damaged by the effect of blasting energy. Insignificant damage is however observed in rock mass closed to the existing tunnel.

9. ACKNOWLEDGEMENTS

This work was supported by the Vietnamese Ministry of Education and Training, under the B2016-MDA-10ĐT research project. The authors wish to thank Mr. Clement Baumont for giving the field testes.

10. REFERENCES

- [1] Abaqus, 2011. User's Examples and Theor Manual, Version 6.10, Simulia, Providence.
- [2] Smith, P. D., Vismeg, P., Teo, L.C.L., Tingey, 1998. Blastwave transmission along rough-walled tunnels. *Int. J. Impact Engng* Vol. 21, No. 6, pp. 419-432.
- [3] Khosrow Bakhtar., 1997. Impact of joints and discontinuities on the blast-response of responding tunnels studied under physical modeling at 1-g. *Int. J. Rock Mech. & Min. Sci.* 34:3-4, paper No. 021.
- [4] Pao, Y.H., 1983. Elastic waves in solids. *Journal of Applied Mechanics* 50 (4), 1152-1164.
- [5] Wersall, C, 2008. Blast-Induced Vibrations and Stress Field Changes around circular tunnels. Master of Science Thesis 08/04. Division of Soil and Rock Mechanics.
- [6] Li, J.C., Li, H.B., Ma, G.W., Zhou, Y.X., 2013. Assessment of underground tunnel stability to adjacent tunnel explosion. *Tunneling and Underground Space Technology* 35, 227-234.

- [7] Ansell, A., 2004. In situ testing of young shotcrete subjected to vibration from blasting Tunneling and Underground Space Technology 19, 587–593.
- [8] Ozer, U., 2008. Environmental impacts of ground vibration induced by blasting at different rock units on the Kadikoy–Kartal metro tunnel. Engineering Geology 100, 82–90.
- [9] Nateghi, R., 2011. Prediction of ground vibration level induced by blasting at different rock units. International Journal of Rock Mechanics and Mining Sciences 48, 899–908.
- [10] Nateghi, R., Kiany, M., Gholipouri, O., 2009. Control negative effects of blasting waves on concrete of the structures by analyzing of parameters of ground vibration. Tunneling and Underground Space Technology 24, 508–515.
- [11] Lin, D., 2011. The mitigation negative effect of tunnel-blasting-induced vibrations on existing tunnel and buildings. Journal of coal science & engineering. Vol.17 No.1, 28–33.
- [12] Jiang, L.C., Hu, L.Q., Lai, X.Y., 2011. Investigation on the threshold control of safety blasting vibration velocity for the extraction of complicated orebody under railway. Mining Science and Technology (China) 21, 169–174.
- [13] Wu, Ch., Lu, Y. and Hao, H., 2004. Numerical prediction of blast-induced stress wave from large-scale underground explosion. Int. J. Numer. Anal. Meth. Geomech, 28, 93-109.
- [14] Saharan, M. R. and Mitri, H. S., 2008. Numerical Procedure for Dynamic Simulation of Discrete Fractures Due to Blasting. Rock Mech. Rock Engng, 41 (5), 641-670.
- [15] Park, D., Byungkyu Jeon, Seokwon Jeon, 2009. A Numerical Study on the Screening of Blast-Induced Waves for Reducing Ground Vibration, Rock Mech Rock Eng 42, 449-473.
- [16] Jong-Ho Shin, Hoon-Gi Moon, Sung-Eun Chae., 2011. Effect of blast-induced vibration on existing tunnels in soft rocks. Tunnelling and Underground Space Technology 26, 51-61.
- [17] Buonsanti, M., Leonardi, G., 2013. 3-D simulation of tunnel structures under blast loading. Archives of civil and mechanical engineering, 124-128.
- [18] Liang, Q. Jie Li, Dewu Li, Erfeng Ou., 2013. Effect of Blast-Induced Vibration from New Railway Tunnel on Existing Adjacent Railway Tunnel in Xinjiang, China. Rock Mech Rock Eng 46, 19-39.
- [19] Xia, X., Li, H.B., Li, J.C., Liu, B., Yu, C., 2013. A case study on rock damage prediction and control method for underground tunnels subjected to adjacent excavation blasting. Tunnelling and Underground Space Technology, No 35, 1–7.
- [20] Yang, J., Lu, W., Chen, M., Zhou, Ch., 2012. Microseism Induced by Transient Release of In Situ Stress During Deep Rock Mass Excavation by Blasting. Rock Mechanics and Rock Engineering 46(4), 859–875.
- [21] Lua, W., Yang, J., Chen, M., Zhou, C., Yi Luo, Jin, L., 2012. Dynamic response of rock mass induced by the transient release of in-situ stress. International Journal of Rock Mechanics & Mining Sciences 53, 129–141.
- [22] Dang, V.K., Huang, G.J., Vu, X.H., Pellet, F.L., 2012. Experimental and numerical investigations of the Split Hopkinson test on granite rock. Proceeding of the international conference on advances in mining and tunneling. 20-21 August 2012, Hanoi, Vietnam.
- [23] Pellet, F. L., Dang, V.K., Baumont, C., Dusseux, M., Huang, G. J., 2013. Determination of dynamic rock strength to assess blasting efficiency. Eurock. 21-26 September 2013, Wroclaw, Poland.
- [24] Konya CJ, Walter EJ, 1991. Rock blasting and overbreak control. FHWA-HI-92-00, National Highway Institute, 5 pp.
- [25] Olsson, M., Nie, S., Bergqvist, I., Ouchterlony, F., 2001. What causes cracks in rock blasting. In: Proc. EXPLO2001. Hunter Valley, NSW, Australia, 191–196.
- [26] Biggs, J. M., 1964. Introduction to Structural Dynamics. New York, McGraw-Hill.
- [27] DIN4150 Part 3, 1986. Erchütterungen im Bauwesen – Einwirkungen auf bauliche Anlagen.
- [28] Par Chong Zhang, 2013. Seismic Safety Evaluation of Concrete Dams: A Nonlinear Behavioral Approach, USA.
- [29] Agne Rustan, 1998. Rock Blasting Terms and Symbols: A Dictionary of Symbols and Terms in Rock Blasting and related areas like drilling, mining and rock mechanics. Rotterdam. ISBN 9054104414.
- [30] Song, G., Shi, X., Chen, S., 2006. New method for determining blasting vibration damage criterion on open-pit slope and its application. Journal of Central South University of Technology, No 36, 485-488.
- [31] Dey, K. and Murthy, V.M.S.R., 2012. Prediction of blast-induced overbreak from uncontrolled burn-cut blasting in tunnels driven through medium rock class. Tunnelling and Underground Space Technology, No 28, 49–56.
- [32] Yang, H., Lu, W.B., Zhao, Z.G., Yan, P., Chen, M. Safety distance for secondary shotcrete subjected to blasting vibration in Jinping-II deep-buried tunnels. Tunnelling and Underground Space Technology 43 (2014) 123–132.
- [33] X.F. Deng, J.B. Zhu, S.G. Chen, Z.Y. Zhao, Y.X. Zhou, J. Zhao. Numerical study on tunnel damage subject to blast-induced shock wave in

- jointed rock masses. *Tunnelling and Underground Space Technology* 43 (2014) 88–100.
- [34] Dang, V.K., 2016. The effect of length of 3D model on result of model during study the effect of blast vibration on adjacent existing tunnel lining. *Mining and Industry Journal*, ISSN 0868-7052, 2, 32-37, 2016.
- [35] Dang, V.K., 2016. Numerical Simulation of Wave Propagation in Rock Media: The Effect of Element Type on the Boundary Condition and the Analysis Result in a Model of Blast Vibration, *Journal of Mining and Earth Sciences*, 54, 3, 17-25, 2016. ISSN 1859-1469.
- [36] Nesvijski, E. G., 2009. On a Possibility of Rayleigh Transformed Sub-Surface Waves Propagation. *The e-Journal of Nondestructive Testing & Ultrasonics*. Issue Vol. 5 No. 9.

Copyright © Int. J. of GEOMATE. All rights reserved, including the making of copies unless permission is obtained from the copyright proprietors.
